

## Detecting Ligand Binding to a Small RNA Target via Saturation Transfer Difference NMR Experiments in D<sub>2</sub>O and H<sub>2</sub>O

Moriz Mayer and Thomas L. James\*

Department of Pharmaceutical Chemistry, University of California, San Francisco, California 94143-0446

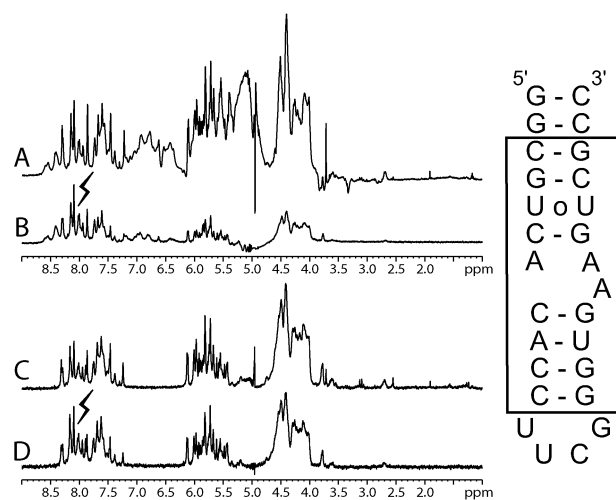
Received July 1, 2002

Although the mechanism of action of clinically important antibiotics entails binding to ribosomal RNA,<sup>1</sup> RNA has in the past not been targeted systematically for drug development. However, this situation is changing. One reason for this is the increased understanding of structural and energetic characteristics of binding processes, with more 3D structures of RNA alone and in complexes with both proteins and ligands being reported.<sup>2</sup> Targeting RNA gives drug developers a different approach to fight pathogens and diseases.<sup>3</sup>

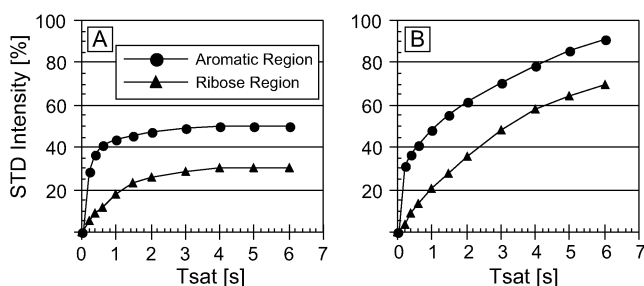
Use of saturation transfer difference (STD) NMR to detect and characterize the binding of low molecular weight compounds to proteins has found utility in recent years.<sup>4</sup> Until now, however, there has been little effort to target RNA in STD NMR experiments to detect small molecule interactions.<sup>5</sup> For this study, a small RNA (27-nucleotide; 9 kDa) was selected explicitly to challenge the methodology. The short correlation time  $\tau_c$  inherent to a molecule this size leads to slow spin diffusion rates in the target and reduced saturation transfer to the bound ligand. The reduced proton density in RNA as compared to proteins poses an additional challenge.

Figure 1 shows the secondary structure of the model ribosomal A-site used here. The 3D structure of this RNA alone, as well as complexed to the ligand paromomycin, has been solved by NMR.<sup>6</sup> The asymmetric bulge with the extra adenosine residue is the crucial motif for ligand specificity. The reference (A, C) and STD NMR (B, D) spectra in H<sub>2</sub>O and D<sub>2</sub>O, respectively, of A-site RNA are displayed in Figure 1. A band-selective saturation pulse was used here, which results in a higher S/N ratio as compared to single Gaussian pulses.<sup>7</sup> To reduce molecular motion, all experiments were performed at 10 °C. Good results are obtained with the irradiation frequency at 8.1 ppm, which is made apparent by comparing relative intensities of the reference and STD NMR spectra. Many exchangeable and nonexchangeable base protons resonate in this region and are consequently saturated directly. Magnetization spreads into all spectral regions during the 4-s saturation time although with different efficiencies in D<sub>2</sub>O and H<sub>2</sub>O, respectively.

Figure 2 shows the STD signal intensity buildup of two spectral regions of RNA in H<sub>2</sub>O (A) and D<sub>2</sub>O (B) with increasing saturation periods. The circles represent the saturation time profile for the region from ca. 7.5–8.5 ppm, whereas the triangles correspond to the region from 4 to 4.6 ppm. The saturation time experiments in D<sub>2</sub>O reveal that the intensities have not reached their maximum even at a saturation time of 6 s. In H<sub>2</sub>O, in contrast, the STD effect has already reached its maximum after 3 s of saturation. Another observation is that the STD signal intensity is much reduced in the STD spectra recorded in H<sub>2</sub>O. The STD effect levels off at 50% for the base proton region and at 30% for the ribose proton region. The STD effect in D<sub>2</sub>O for the same regions reaches values of 90



**Figure 1.** (A, C) Reference and (B, D) STD NMR spectra of 0.1 mM A-site rRNA in H<sub>2</sub>O (A, B) and D<sub>2</sub>O (C, D); 256 and 64 scans were acquired for the STD spectra B and D. STD NMR spectra were irradiated at 8.1 ppm as indicated by the arrow. The secondary structure of the model A-site RNA is also displayed with the boxed residues corresponding to the natural A-site.



**Figure 2.** Plots showing the STD signal intensity of two spectral regions of the RNA. (A) and (B) correspond to signal intensities recorded in H<sub>2</sub>O and D<sub>2</sub>O, respectively. Circles indicate intensities of the directly saturated aromatic proton region of 7.5–8.5 ppm, and triangles reflect the ribose proton region from 4 to 4.6 ppm.

and 70%, respectively. One can also observe that about 25% of the base proton intensity in the STD spectrum is due to the direct saturation at 8.1 ppm, which is present immediately and does not need to be transferred by spin diffusion. This can be seen by the initial jump with only 0.2 s saturation.

The source for the reduced STD signal intensity in H<sub>2</sub>O is the enhanced longitudinal relaxation rate  $R_1$ . The larger  $R_1$  is, the faster a steady state between saturation and relaxation is reached. The data presented here exemplify this effect. In H<sub>2</sub>O,  $R_1$  is larger because water protons provide a rich source of unsaturated protons serving as a relaxation sink. This process is effective because both the minor and the major grooves of the RNA are hydrated.<sup>8</sup> In

\* To whom correspondence should be addressed. E-mail: james@picasso.ucsf.edu.

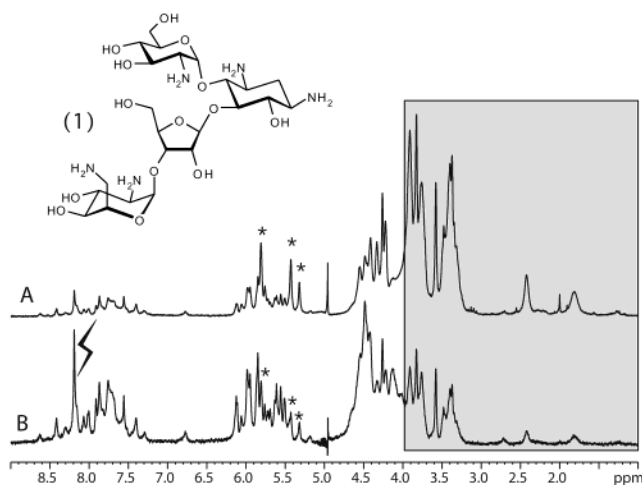


**Figure 3.** (A) Reference and (B) STD NMR spectra of 0.1 mM RNA in the presence of 1.5 mM paromomycin (1); 256 scans were acquired for the STD spectrum. The arrow indicates the irradiation frequency at 8.1 ppm. Asterisks indicate the anomeric proton resonances of paromomycin. In the shaded region, all but three resonances originate from the ligand.

addition, exchanging amino, imino, and hydroxyl protons leads to magnetization losses.

STD experiments with small RNA targets in D<sub>2</sub>O should be performed with saturation periods of 4 s or more, whereas in H<sub>2</sub>O, ca. 2 s is sufficient due to larger  $R_1$  values. In general, it will be more practical to use D<sub>2</sub>O in STD NMR experiments with small RNA targets, because an extra spectral window from ca. 6.0–7.3 ppm is available for observing ligands and the STD spectral intensities can be larger.

The STD technique works most readily with rapidly exchanging ligands.<sup>4b</sup> We expressly chose to demonstrate the methodology with a more challenging system entailing a ligand that exchanges slowly. We prepared a D<sub>2</sub>O sample of 0.1 mM RNA and 15-fold excess of paromomycin (1). The aminoglycoside binds A-site RNA with  $K_D = 0.2 \mu\text{M}$ . For NMR-based screening, this corresponds to a high affinity interaction. Because of slow exchange between bound and free species, only small STD signals are expected.

Figure 3 shows reference (A) and STD NMR (B) spectra. In the shaded region of the spectra, all but three resonances correspond to the ligand (cf. Figure 1). The asterisks mark three anomeric proton signals of (1) at 5.3, 5.4, and 5.8 ppm. Any small molecule signal in the STD spectrum results from that molecule binding to the receptor. The STD spectrum in Figure 3B clearly shows signals from the drug, demonstrating binding. In spectral regions with overlapping signals, differentiation between RNA and ligand STD signals becomes more difficult. Also, both ligand and RNA signals show exchange broadening, further reducing resolution. Use of higher ligand excess is of advantage here because it leads to sharper signals of the exchange broadened ligands. We have unpublished results showing that differentiation between ligand and RNA STD signals is more straightforward with weaker affinity ligands. Under those conditions, the ligand STD signals reach higher values and are therefore easily identified. We have also tested this system with up to 10% deuterated DMSO, and no negative effects on the STD spectra were detected. Using a relaxation filter to reduce or eliminate RNA background signals, useful in STD NMR experiments with proteins,<sup>4a,b</sup> is not feasible for this small RNA because the  $T_{1\rho}$  values are too long.

Similar sensitivity reductions and/or background signals of the RNA are experienced in most of the ligand-based NMR screening experiments because, ultimately, the small size and low proton density of the RNA result in long  $T_{1\rho}$  values and a reduced intermolecular cross-relaxation rate. The consequence is that the ligand excess region in which WaterLOGSY or diffusion NMR experiments are possible is equally reduced. Because high ligand excess does not lead to false negatives in STD experiments, it is possible to use a larger excess to observe sharper lines for exchange-broadened signals. What holds true for any type of NMR screening experiment is that once the system is optimized for a specific ligand, competition experiments can provide a simple indicator for binding effects and for calculating affinities.<sup>4b,5d</sup>

In conclusion, we demonstrated that a D<sub>2</sub>O solution is preferable for STD NMR experiments with small RNA targets due to reduced  $R_1$  rates and the extra spectral window available from ca. 6.0–7.3 ppm. Furthermore, binding of the high affinity ligand paromomycin was easily detected from the STD spectra. As with other NMR screening procedures, this method has advantages relative to most other non-NMR screening methods: observation of a direct effect precludes false positives, and ligands can be identified in a mixture. The main application for these experiments will be low-throughput screening of focused libraries in drug discovery and optimization.

**Acknowledgment.** This work has been supported by a fellowship to M.M. from the DAAD and by an NIH grant AI46967 and an American Foundation for AIDS Research grant 02881-31-RGT to T.L.J. The authors also thank J. Puglisi and D. Fourmy for providing the chemical shift tables for the A-site RNA.

## References

- (1) Schroeder, R.; Waldsich, C.; Wank, H. *EMBO J.* **2000**, *19*, 1–9.
- (2) (a) Hermann, T. *Angew. Chem., Int. Ed.* **2000**, *39*, 1890–1904. (b) Ogle, J. M.; Brodersen, D. E.; Clemons, W. M., Jr.; Tarry, M. J.; Carter, A. P.; Ramakrishnan, V. *Science* **2001**, *292*, 897–902.
- (3) (a) Lind, K. E.; Du, Z.; Fujinaga, K.; Peterlin, B. M.; James, T. L. *Chem. Biol.* **2002**, *9*, 185–193. (b) DeJong, E. S.; Luy, B.; Marino, J. P. *Curr. Top. Med. Chem.* **2002**, *2*, 289–302. (c) Xin-Shan, Y.; Zhang, L. H. *Curr. Med. Chem.* **2002**, *9*, 929–939.
- (4) (a) Mayer, M.; Meyer, B. *Angew. Chem., Int. Ed.* **1999**, *38*, 1784–1788. (b) Mayer, M.; Meyer, B. *J. Am. Chem. Soc.* **2001**, *123*, 6108–6117. (c) Haselhorst, T.; Weimar, T.; Peters, T. *J. Am. Chem. Soc.* **2001**, *123*, 10705–10714. (d) Jayalakshmi, V.; Krishna, N. R. *J. Magn. Reson.* **2002**, *155*, 106–118.
- (5) (a) Ramos, A.; Kelly, G.; Hollingworth, D.; Pastore, A.; Frenkiel, T. *J. Am. Chem. Soc.* **2000**, *122*, 11311–11314. (b) Lane, A. N.; Kelly, G.; Ramos, A.; Frenkiel, T. A. *J. Biomol. NMR* **2001**, *21*, 127–139. (c) Dalvit, C.; Pevarello, P.; Tato, M.; Veronesi, M.; Vulpetti, A.; Sundstrom, M. *J. Biomol. NMR* **2000**, *18*, 65–68. (d) Dalvit, C.; Flocco, M.; Knapp, S.; Mostardini, M.; Perego, R.; Stockman, B. J.; Veronesi, M.; Varasi, M. *J. Am. Chem. Soc.* **2002**, *124*, 7702–7709.
- (6) (a) Fourmy, D.; Recht, M. I.; Blanchard, S. C.; Puglisi, J. D. *Science* **1996**, *274*, 1367–1371. (b) Lynch, S. R.; Recht, M. I.; Puglisi, J. D. *Methods Enzymol.* **2000**, *317*, 240–261. (c) Recht, M. I.; Fourmy, D.; Blanchard, S. C.; Dahlquist, K. D.; Puglisi, J. D. *J. Mol. Biol.* **1996**, *262*, 421–436.
- (7) All NMR experiments were performed on a 500 MHz Bruker spectrometer equipped with a triple resonance cryoprobe. 100  $\mu\text{M}$  A-site RNA was dissolved in 0.5 mL of 20 mM phosphate-buffered D<sub>2</sub>O or H<sub>2</sub>O/D<sub>2</sub>O 9:1, adjusted to pH 6.8, containing 50 mM NaCl. Temperature was set to 10 °C, and unless indicated otherwise the saturation time was 4 s. A G4 Gaussian cascade pulse of 20 ms with an excitation bandwidth of ca. 0.8 ppm was used. A single Gaussian pulse of the same duration has an excitation profile of ca. 0.2 ppm. The WATERGATE STD pulse program in ref 4b was used in all experiments.
- (8) (a) Conte, M. R.; Conn, G. L.; Brown, T.; Lane, A. N. *Nucleic Acids Res.* **1996**, *24*, 3693–3699. (b) Egli, M.; Portmann, S.; Usman, N. *Biochemistry* **1996**, *35*, 8489–8494.

JA027526Z